Journal of Thermal Analysis and Calorimetry (2019) 135:3247–3257
https://doi.org/10.1007/s10973-018-7471-9

Turbulent combined forced and natural convection of nanofluid in a 3D rectangular channel using two-phase model approach

Hossein Esmaeili[1] · T. Armaghani[2] · A. Abedini[3] · I. Pop[4]

Received: 23 April 2018 / Accepted: 5 June 2018 / Published online: 18 June 2018

Abstract

The nanofluid is a mixture of base fluid and solid nanoparticles in nanosize. The heat transfer generated by the nanofluid is more than the base fluid and its lowering pressure drop, which is why its use is increasing. In this paper, the effect of volume fraction, aspect ratio and diameter of the nanoparticles on the turbulent mixed convection in a three-dimensional rectangular channel is numerically investigated. The boundary conditions are constant heat flux, and governing equations are numerically solved by the mixture model. Base fluid in this study, water and aluminum oxide are used as nanoparticles. In this study, all physical properties are considered constant and the effects of volume fraction, aspect ratio and diameter of the particles on the thermal and hydrodynamic parameters of the fluid were studied.

Keywords Nanofluid · Mixed convection · Turbulent flow · Three dimensional · Rectangular channel

List of symbols

a	Acceleration
AR	Aspect ratio
C_p	Heat capacity
$(C_p)_{eff}$	Effective heat capacity of nanofluid
d_h	Hydraulic diameter
d_p	Particles diameter
d_f	Diameter of nanofluid
f_{drag}	Drag function
g	Gravitational acceleration
g_i	Gravitational acceleration in x-, y- and z-directions
h_k	Sensible enthalpy of the k-phase
k_b	Boltzmann constant
k_{eff}	Effective thermal conductivity of nanofluid
k_p	Thermal conductivity of particles
k_f	Thermal conductivity of fluid
L	Length of channel
l_{bf}	Length of free path
Nu	Local Nusselt number, hd_h/k
p	Fluid pressure
q_w	Wall heat flux
P_o	Static pressure
Pr	Prandtl number
Re	Reynolds number
Ri	Richardson number, Gr/Re^2
T	Temperature
T_i	Inlet temperature
T_o	Reference temperature
T^*	Dimensionless temperature
T'	Fluctuating temperature
V_B	Brownian speed
V_{dr}	Spin velocity
V_f	Velocity of base fluid
V_k	Velocity of the k-phase
V_x, V_y, V_z	Velocity components in x-, y- and z-directions
V_m	Mean mass velocity
V'	Fluctuating velocity
V_p	Speed of particles
V_o	Velocity in z-direction
x, y, z	Cartesian coordinates

Greek symbols

α_T	Thermal diffusivity
β	Thermal expansion coefficient (K^{-1})

✉ I. Pop
popm.ioan@yahoo.co.uk

[1] Department of Chemical Engineering, Bushehr Branch, Islamic Azad University, Bushehr, Iran

[2] Department of Engineering, Mahdishahr Branch, Islamic Azad University, Mahdishahr, Iran

[3] Department of Engineering, Semnan Branch, Islamic Azad University, Semnan, Iran

[4] Department of Mathematics, Babeş-Bolyai University, 400084 Cluj-Napoca, Romania

β_{eff} Effective thermal expansion coefficient
β_f Thermal expansion coefficient of base fluid
β_{nf} Thermal expansion coefficient of nanofluid
ϕ_k Volume fraction of the *k*-phase
ϕ_p Volume fraction of particles
μ_{eff} Effective viscosity
μ_{nf} Nanofluid viscosity
μ_f Viscosity of base fluid
ρ_{eff} Effective nanofluid density
ρ_f Density of basic fluid
ρ_k Density of the *k*-phase density of the mixture (kg m^{-3})
ρ_m Density of the mixture (kg m^{-3})
ρ_p Density of particles
∇ Gradient
τ Shear stress

Introduction

Nanofluid is defined as a fluid, which uses metal or non-metallic particles in nano sizes as nanoparticles in the base fluid. Previously, more research was done to measure and model the thermal conductivity, but in recent years, there has been much research on nanofluid heat transfer. Nanofluid is a fluid with nanoparticles in sizes from 1 to 100 nm, which has a high thermal conductivity and heat transfer coefficient relative to the base fluid.

The idea of adding solid particle in ordinary fluids to increase heat transfer was first proposed by Maxwell [1] about a century ago, but due to the large size of the solid metal particles (in millimeter and microsize), problems such as instability and sedimentation of these particles arose. Choi [2] was the first to use the term nanofluid for a fluid having nanoparticles. He showed that the addition of a small amount of nanoparticles (for example, 1% volume fraction) to the base fluid nearly doubles the thermal conductivity coefficient. Other researchers, including Xuan and Li [3], showed that increasing volume fraction about 1–5% could increase the ratio of effective thermal conductivity to the thermal conductivity of the base fluid by 20%. Wang et al. [4] proposed a model to predict the thermal conductivity of the nanofluid. The model was suitable for low volume fractions of nanofluid with metallic. The comparison of the above model with experimental results in a nanoparticle diameter of 50 nm and a volume fraction of less than 0.05 has an acceptable agreement. Hwang et al. [5] measured the thermal conductivity coefficient of four nanofluid types and showed that the thermal conductivity is linear with the volume fraction of nanoparticles. They also stated that the thermal conductivity measured in the experiments was larger than that obtained from theoretical models, and the thermal conductivity of the nanofluid in comparison with the base fluid in the volume fraction of 1% was 11.3%. Nie et al. [6] examined various mechanisms to increase the thermal conductivity and showed that in a given size of nanoparticles, the thermal conductivity is proportional to temperature and inversely proportional to viscosity. Sankar et al. [7] used a theory based on the molecular dynamics model to estimate the thermal conductivity of the nanofluid. They showed that by increasing the volume fraction from 1 to 7%, the thermal conductivity coefficient increases and the temperature increase also increases the thermal conductivity coefficient. Two approaches based on conservation equations have been adopted in the literature to investigate the numerical heat transfer of nanofluids: single-phase model and two-phase model (see Wang and Mujumdar [8]). In Ghaffari et al. [9], a two-phase numerical study of the thermal and hydrodynamic effects of the turbulent flow of the nanofluid in the curved horizontal tube was performed using a mixture model. They measured numerically the mixed convection of the turbulent flow of nanofluid containing water and aluminum oxide in the inlet region of a curved tube. They also considered the governing equations in the form of three-dimensional cylindrical coordinates. To analyze the thermal and hydrodynamic parameters, they used a mixed multiphase model and also studied the effects of buoyancy force, centrifugal force and the volume fraction of nanoparticles. Their results show that the volume fraction of nanoparticles has no significant effect on the skin friction coefficient, but its effect on the thermal parameters and the turbulence intensity of the flow is high and the results are close to the experimental and numerical work carried out by others. Rostamani et al. [10] investigated numerically the forced convection of the nanofluid through the channel. The studied flow regime was a turbulent and two-dimensional channel, and the assumption of constant thermal heat flux was used on the channel wall. The nanoparticles used were a mixture of copper oxide, titanium oxide and aluminum oxide and water base fluid. The boundary condition of the constant heat flux along the wall was applied, and the thermophysical properties of the temperature-dependent nanofluid were considered. Their results showed that with the increasing of the volume fraction, the shear stress at the wall and the heat transfer rate increased. Also, for a given Reynolds number and volume fraction, the copper oxide nanoparticles improved the heat transfer rate rather than the nanoparticles of aluminum and titanium oxide. Mirmasoumi et al. [11] studied the effect of the average diameter of nanoparticles on the mixed convection heat transfer in a nanomaterial. The geometry studied in this work, the horizontal tube and the nanofluid, was water with aluminum oxide nanoparticles. Flow is a fully developed,

laminar method of solving this problem, and the numerical model used is two-phase mixture model. In this case, it is assumed that constant heat flux is applied along the wall; all the physical properties of the fluid are assumed to be constant, except for the density that changes linearly with temperature. The boundary conditions at the inlet part of the pipe are such that the specified inlet temperature and the input velocity are fixed in the axial direction, and in other directions, zero is considered. Laminar and turbulent mixed convection heat transfer of nanofluids in a rectangular shallow cavity using a two-phase mixture model is studied by Goodarzi et al. [12]. Garoosi et al. [13] studied mixed convection heat transfer of nanofluid in a two-sided lid-driven cavity with several pairs of heaters and coolers inside using two-phase mixture model. Armaghani et al. [14–19] used the Buongiorno two-phase model for modeling the forced convection heat transfer of nanofluid in LNTE and LTE porous channel. Rashidi et al. [20, 21] studied steady two-dimensional, viscous incompressible MHD nanofluid flow. They concluded that the presence of magnetic field leads to decrease the nanofluid velocity and increase the nanofluid temperature. Effects of the external magnetic field on flow and heat transfer are investigated by Sheikholeslami et al. [22, 23]. Their results show that the Nusselt number is an increasing function of the Reynolds number, the nanoparticle volume fraction and the magnetic number. The Euler and mixture two-phase models for turbulent flow of alumina nanofluid inside a horizontal tube are compared by Hejazian et al. [24]. They showed the mixture model was in a better agreement with experimental results for the estimation of average Nusselt number. It is worth mentioning that many references on nanofluids can be found in the books by Das et al. [25], Nield and Bejan [26], and Shenoy et al. [27], and in the review papers by Buongiorno et al. [28], Kakaç and Pramuanjaroenkij [29], Wong and Leon [30], Manca et al. [31], Mahian et al. [32], Sheikholeslami and. Ganji [33], Meyes et al. [34], etc.

The purpose of this study is to investigate the heat transfer and pressure drop of nanofluid in a three-dimensional rectangular channel using two-phase approach. The fluid flow was considered to be turbulent and the effect of parameters such as volume fraction, aspect ratio and diameter of nanoparticles on thermal and hydrodynamic parameters was investigated.

Problem definition and mathematical formulation

Geometry

The geometry studied in this work is a 3D channel with length L, width 2a and height 2b as shown in Fig. 1. The fluid used is the water, and aluminum oxide particles were used as nanoparticles in the base fluid.

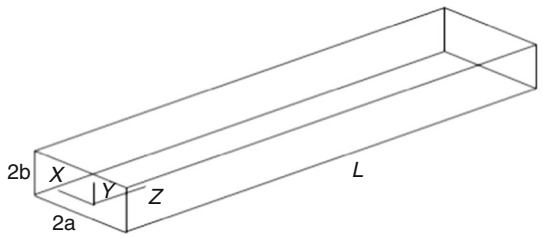

Fig. 1 Geometry of the problem

Governing equations

Continuity equation

The general form of the continuity equation is as follows:

$$\nabla \cdot (\rho_{\mathrm{m}} V_{\mathrm{m}}) = 0. \tag{1}$$

In the above equation, V_{m} is the mean mass velocity of the mixture and ρ_{m} is the density of the mixture as defined below,

$$V_{\mathrm{m}} = \frac{\sum_{k=1}^{n} \phi_{\mathrm{k}} \rho_{\mathrm{k}} V_{\mathrm{k}}}{\rho_{\mathrm{m}}} \;\&\; \rho_{\mathrm{m}} = \sum_{k=1}^{n} \phi_{\mathrm{k}} \rho_{\mathrm{k}}. \tag{2}$$

In the above equation, ϕ_{k} is the volume fraction of the k-phase.

Momentum equation

$$\nabla \cdot (\rho_{\mathrm{m}} V_{\mathrm{m}} V_{\mathrm{m}}) = -\nabla P + \nabla \cdot (\tau - \tau_t) + \nabla \cdot \left(\phi_{\mathrm{k}} \rho_{\mathrm{k}} V_{\mathrm{dr,k}} V_{\mathrm{dr,k}}\right) - \rho_{\mathrm{m}} \beta_{\mathrm{eff}} g (T - T_i) \tag{3}$$

$$\tau = \mu_{\mathrm{eff}} \nabla V_{\mathrm{m}}, \; \tau_t = -\sum_{k=1}^{n} \phi_{\mathrm{k}} \rho_{\mathrm{k}} \overline{V'_{\mathrm{k}} V'_{\mathrm{k}}}. \tag{4}$$

n is the number of secondary phases and V' is the fluctuating velocity. $V_{\mathrm{dr},k}$ is equal to the spin velocity defined for the kth secondary phase as follows:

$$V_{\mathrm{dr,k}} = V_{\mathrm{k}} - V_{\mathrm{m}}. \tag{5}$$

The relative velocity (slip) is defined as the speed of the second phase (particles, p) relative to the velocity of the first phase (base fluid, f), as follows:

$$V_{\mathrm{pf}} = V_{\mathrm{p}} - V_{\mathrm{f}}. \tag{6}$$

Also, the relationship between the spin velocity and slip velocity is as follows:

$$V_{\mathrm{dr,p}} = V_{\mathrm{pf}} - \sum_{k=1}^{n} \frac{\phi_{\mathrm{k}} \rho_{\mathrm{k}}}{\rho_{\mathrm{m}}} V_{\mathrm{fk}}. \tag{7}$$

Finally, the slip or relative velocity between the two phases, which is considered to be the interaction between the two phases, is calculated from the following relation known as Manning's relation (see Nie et al. [6]).

$$V_{\mathrm{pf}} = \frac{\rho_{\mathrm{p}} d_{\mathrm{p}}^2}{18\mu_{\mathrm{f}} f_{\mathrm{drag}}} \frac{(\rho_{\mathrm{p}} - \rho_{\mathrm{m}})}{\rho_{\mathrm{p}}} a. \tag{8}$$

In the above relation, f is the drag function, which is derived from the relation of Schiller and Neumann [31]:

$$f_{\mathrm{drag}} = \begin{cases} 1 + 0.15 Re_{\mathrm{p}}^{0.687}, & Re_{\mathrm{p}} \le 1000 \\ 0.0183 Re_{\mathrm{p}}, & Re_{\mathrm{p}} \ge 1000 \end{cases}. \tag{9}$$

In this case, Re_{p} and acceleration a are defined as follows:

$$a = g - (V_{\mathrm{m}} \cdot \nabla) V_{\mathrm{m}} \tag{10}$$

$$Re_{\mathrm{P}} = \frac{V_{\mathrm{m}} d_{\mathrm{p}}}{v_{\mathrm{eff}}}. \tag{11}$$

Second-phase volume fractional equation

The second-phase fractional equation for the two-phase flow is as follows:

$$\nabla \cdot (\phi_{\mathrm{p}} \rho_{\mathrm{p}} V_{\mathrm{m}}) = -\nabla \cdot (\phi_{\mathrm{p}} \rho_{\mathrm{p}} V_{\mathrm{dr,p}}). \tag{12}$$

Energy equation

$$\nabla \cdot \sum_{k=1}^{n} (\phi_{\mathrm{k}} V_{\mathrm{k}} (\rho_{\mathrm{k}} E_{\mathrm{k}} + P)) = \nabla \cdot \left(k_{\mathrm{eff}} \nabla T - C_{\mathrm{p}} \rho_{\mathrm{m}} \overline{V' T'} \right), \tag{13}$$

where k_{eff} is the effective thermal conductivity of the nanofluid and T' is the fluctuating temperature. E_{k} in the above relationship is defined as follows:

$$E_{\mathrm{k}} = h_{\mathrm{k}} - \frac{P}{\rho_{\mathrm{k}}} + \frac{V_{\mathrm{k}}^2}{2}, \tag{14}$$

where h_{k} in the above equation is the sensible enthalpy of the k-phase.

Turbulence model

The simplest "complete models" of turbulence are two-equation models in which the solution of two separate transport equations allows the turbulent velocity and length scales to be independently determined. The standard $k - \varepsilon$ model falls within this class of turbulence model and has become the workhorse of practical engineering flow calculations. In this work, the turbulent flow is modeled by the of the two-equation $k - \varepsilon$ model of Shah and London [35].

In this model, the turbulent kinetic energy equation is as follows:

$$\nabla \cdot (\rho_{\mathrm{m}} V_{\mathrm{m}} k) = \nabla \cdot \left(\frac{\mu_{\mathrm{t,m}}}{\sigma_k} \nabla k \right) + G_{\mathrm{k,m}} - \rho_{\mathrm{m}} \varepsilon + G_{\mathrm{b}}. \tag{15}$$

Also, the energy dissipation rate of the turbulent kinetic energy is as follows:

$$\nabla \cdot (\rho_{\mathrm{m}} V_{\mathrm{m}} \varepsilon) = \nabla \cdot \left(\frac{\mu_{\mathrm{t,m}}}{\sigma_\varepsilon} \nabla \varepsilon \right) + \frac{\varepsilon}{K} (c_1 G_{\mathrm{k,m}} - c_2 \rho_{\mathrm{m}} \varepsilon). \tag{16}$$

In the above relationships, the terms and constants are defined as follows:

$$\mu_{\mathrm{t,m}} = \rho_{\mathrm{m}} c_\mu \frac{k^2}{\varepsilon}, \quad G_{\mathrm{k,m}} = \mu_{\mathrm{t,m}} \left(\nabla V_{\mathrm{m}} + (\nabla V_{\mathrm{m}})^T \right), \quad G_{\mathrm{b}} = \beta g_{\mathrm{i}} \alpha_{\mathrm{T}} \mu_{\mathrm{t}} \frac{\partial T}{\partial x_{\mathrm{i}}} \tag{17}$$

$$c_1 = 1.44, \quad c_2 = 1.92, \quad c_\mu = 0.09, \quad \sigma_{\mathrm{k}} = 1, \quad \sigma_\varepsilon = 1.3. \tag{18}$$

Physical properties

Effective nanofluid density (see Baqaie et al. [16]):

$$\rho_{\mathrm{eff}} = (1 - \phi) \rho_{\mathrm{f}} + \phi \rho_{\mathrm{p}}. \tag{19}$$

Nanofluid thermal capacity (see Baqaie et al. [16]):

$$(C_{\mathrm{p}})_{\mathrm{eff}} = \left[\frac{(1 - \phi)(\rho C_{\mathrm{p}})_{\mathrm{f}} + \phi (\rho C_{\mathrm{p}})_{\mathrm{p}}}{\rho_{\mathrm{eff}}} \right]. \tag{20}$$

Thermal conductivity coefficient:

Kahn et al. [2], who considered the Brownian motion and the mean diameter of the nanoparticles, obtained the thermal conductivity of the nanofluid as follows:

$$\frac{k_{\mathrm{eff}}}{k_{\mathrm{f}}} = 1 + 64.7 \times \phi^{0.746} \left(\frac{d_{\mathrm{f}}}{d_{\mathrm{p}}} \right)^{0.369} \left(\frac{k_{\mathrm{p}}}{k_{\mathrm{f}}} \right)^{0.746} \times Pr^{0.9955} \times Re^{1.2321}. \tag{21}$$

In the above relationships, the terms and constants are as follows:

$$Pr = \frac{\mu_{\mathrm{f}}}{\rho_{\mathrm{f}} \alpha_{\mathrm{f}}} \tag{22}$$

$$Re = \frac{\rho_{\mathrm{f}} B_{\mathrm{c}} T}{3\pi \mu^2 l_{\mathrm{bf}}} \tag{23}$$

$$\mu = A \times 10^{\frac{B}{T - C}}, \quad C = 140 \text{ K}, \quad B = 247 \text{ K}, \quad A = 2.414 \times 10^{-5} (\text{Pa s}), \quad B_{\mathrm{c}} = 1.3807 \times 10^{-23} \left(\frac{J}{K} \right). \tag{24}$$

Viscosity:

The effective viscosity of the nanofluid from Mirmasoumi et al.'s relationship (see Mirmasoumi and Behzadmehr [11]), which is a function of temperature, mean diameter of nanoparticles, the volume fraction of nanoparticles, nanoparticle density and physical properties of the base fluid, is obtained as follows:

$$\mu_{\mathrm{nf}} = \mu_{\mathrm{f}} + \frac{\rho_{\mathrm{p}} V_{\mathrm{B}} d_{\mathrm{f}}^2}{72 C \delta}, \tag{25}$$

where the V_{B} of the Brownian Speed and δ is obtained from the following equation:

$$V_{\mathrm{B}} = \frac{1}{d_{\mathrm{p}}} \sqrt{\frac{18 k_{\mathrm{b}} T}{\pi \rho_{\mathrm{p}} d_{\mathrm{p}}}} \tag{26}$$

$$\delta = \sqrt[3]{\frac{\pi}{6\phi}} d_{\mathrm{p}} \tag{27}$$

and C in Eq. (25) is obtained from the following equation:

$$C = \mu_{\mathrm{f}}^{-1} \left[(c_1 d_{\mathrm{p}} + c_2)\phi + (c_3 d_{\mathrm{p}} + c_4) \right]. \tag{28}$$

It should be noted that in the equation above the constants are considered as follows:

$$\begin{aligned} C_1 &= -0.113 \times 10^{-5}, \quad C_2 = -0.277 \times 10^{-5}, \\ C_3 &= -0.09 \times 10^{-5}, \quad C_4 = -0.039 \times 10^{-5}. \end{aligned} \tag{29}$$

Volumetric expansion coefficient:

The thermal expansion coefficient of the nanofluid is obtained from the following equation (see Schiller and Neumann [36]):

$$\beta_{\mathrm{nf}} = \left[\frac{1}{1 + \frac{(1-\phi)\rho_{\mathrm{f}}}{\phi \rho_{\mathrm{s}}} \frac{\beta_{\mathrm{s}}}{\beta_{\mathrm{f}}}} + \frac{1}{1 + \frac{\phi}{1-\phi} \frac{\rho_{\mathrm{s}}}{\rho_{\mathrm{f}}}} \right] \beta_{\mathrm{f}}. \tag{30}$$

Boundary conditions

Inlet BCs:

$$V_x = V_y = 0, \quad V_z = V_0 \ \& \ T = T_0.$$

For turbulent the below condition is used:

$$k = \frac{3}{2}(I V_0)^2, \quad \varepsilon = C_{\mu}^{0.75} \frac{K^{1.5}}{0.1 D_{\mathrm{h}}}, \quad C_{\mu} = 0.09, \tag{31}$$

where $I = 0.16 Re^{-\frac{1}{8}}$.

Wall BCs:

$$\begin{aligned} -k_{\mathrm{eff}} \frac{\partial T}{\partial n} &= q_{\mathrm{w}} \\ V_{\mathrm{x}} = V_{\mathrm{y}} = V_{\mathrm{z}} &= 0 \end{aligned} \tag{32}$$

and below for turbulent:

$$k = 0, \varepsilon = 0.$$

Outlet BCs:

In the channel outlet (z = 100), the static pressure is assumed to be p_0, and also the mass balance is used.

Numerical method and validation

Figure 2 shows the grid of the channel, which is denser in the boundary of the entrance and near the walls due to the high gradient of the speed and the network temperature. The finite volume method was used to discretize the governing equations, and SIMPLEC algorithm was used for velocity and pressure coupling. Also, the second-order upwind scheme has been used for modeling convection terms. The simulation of the nanofluid is carried out using finite volume method. Two-equation $K - \varepsilon$ model is used for modeling turbulence. In this work, the grid sensitivity study of the results was investigated by applying different mesh. The results of this study were in the aspect ratio of 1 and volume fraction of 3% and other fixed parameters appeared in Table 1:

The grid study is appeared in Table 2.

Therefore, the number of nodes in different directions is 30 × 60 × 30.

Table 3 shows time of running for the different above-mentioned fixed parameters coding in computer with RAM 4.00 GB and CPU core i3 2.73 GH characteristics (Fig. 2).

Results and discussion

In this work, the modeling of the turbulent flow of aluminum oxide nanofluid was done in a rectangular channel in the three-dimensional model. In this study, the effect of different parameters such as volume fraction, aspect ratio and diameter of nanoparticles on thermal and hydrodynamic parameters such as Nusselt number and friction coefficient was investigated. The results of this research are shown in Figs. 3 and 4. In order to study and validate the solving method, the Nusselt number obtained from this work was compared with the Ditos–Bolter [37] relationship as well as the Darcy friction coefficient with a maximum error value of almost 9% (see Cebeci and Cousteix [38], for example). It should be noted that this comparison is carried out for pure water flow for forced convection.

Table 1 Fixed parameters for grid study

ϕ	AR	Re	Gr	Pr	Ri
0.03	1	40,000	16×10^6	7.997	0.01

Table 2 Grid sensitivity study

Number of nodes $Z \times Y \times X$	$\frac{T_b}{T_i}$	$\frac{V}{V_i}$
5 × 5 × 5	1.04151	1.0974
5 × 5 × 15	1.03834	1.1274
5 × 5 × 30	1.03787	1.1294
5 × 5 × 60	1.03762	1.1301
5 × 15 × 60	1.09806	0.21209
5 × 30 × 60	1.05308	0.50578
5 × 60 × 60	1.05183	0.6738
5 × 30 × 60	1.17562	0.10072
15 × 30 × 60	1.13694	0.32218
30 × 30 × 60	1.0668	0.71281
60 × 30 × 60	1.05432	0.77935

Table 3 CPU time for different *Ri*

Ri	1	0.1	0.01	0.001
CPU time (s)	2100	1620	1260	1080

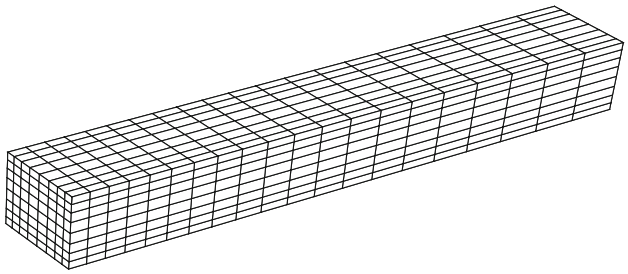

Fig. 2 Channel variable grid

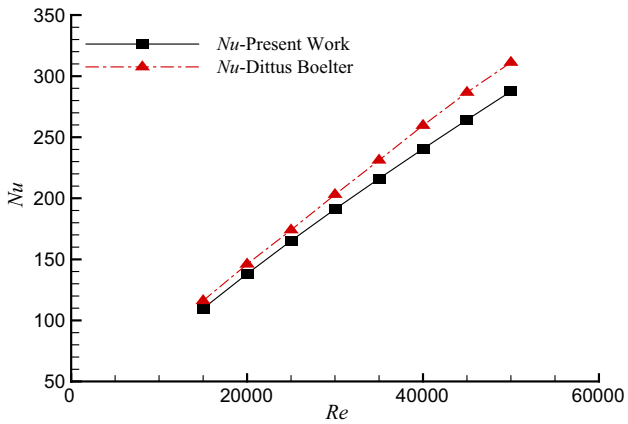

Fig. 3 Comparison of Nusselt number obtained from modeling with Ditos–Bolter model in different Reynolds number

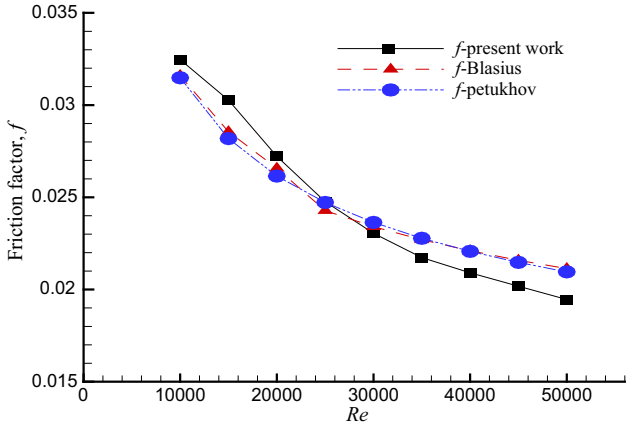

Fig. 4 Comparison of friction coefficient with methods of Belazius and Putukhov for different Reynolds number

Volume fraction effect on heat transfer

In this section, the effect of a change in the nanoparticle volume fraction on the forced convection heat transfer of the turbulent flow of nanofluid of aluminum oxide water into a rectangular channel and in the conditions of Re = 50,000, Ri = 0.01, AR = 0.75, D_h = 0.01 m, L/D_h = 100 was investigated. For this purpose, the volume fraction of nanoparticles containing 0, 1, 3 and 5% of aluminum oxide nanoparticles in water was used. The diameter of the aluminum oxide nanoparticles used in this study is 28 nm. The physical properties of the aluminum oxide nanoparticles and of the water base fluid are considered for the inlet temperature (T_i = 20 °C). Given that the physical properties of the nanofluid are a function of the volume fraction of nanoparticles, for each volume fraction, the physical properties of the fluid change. Figure 5 shows the profile of

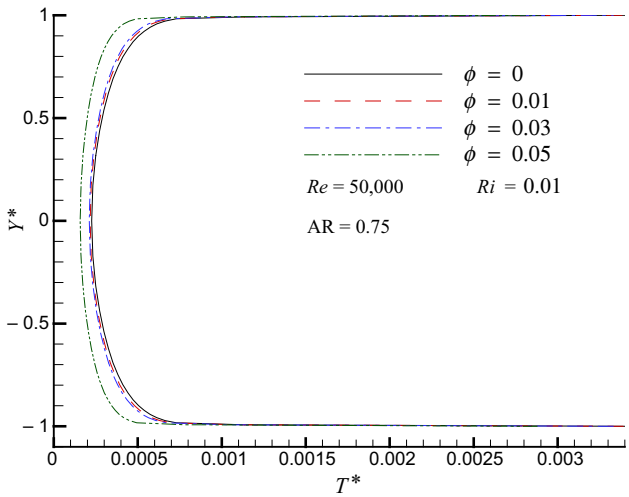

Fig. 5 Dimensionless temperature on a line perpendicular to the channel axis for L/D_h = 100

non-dimensional temperature variation. It should be noted that the dimensionless temperature is defined as follows:

$$T^* = \frac{T - T_i}{\left(\frac{q_w d_h}{k_{eff}}\right)}. \quad (33)$$

By increasing the volume fraction of nanoparticles in a given Reynolds and Richardson numbers, the constant thermal fluxes on the walls and the conduction heat transfer coefficient increase, and the effect of these results will lead to a decrease in the non-dimensional temperature, with the minimum amount of non-dimensional temperature at the channel center and its maximum value occurred near the walls.

The following non-dimensional axial velocity changes in different volume fraction of nanoparticles on an imaginary line perpendicular to the axis of the channel at the point $z = 80$ are shown in Fig. 6. In this figure, it can be seen that due to the increase in the volume fraction, the dimensionless axial velocity changes are not significant; this is due to the fact that the hydrodynamic development depends on Reynolds number, and in all the fractional volumes used in this section, the Reynolds number is constant, so the axial speed profiles will coincide. That is, in fact, with the increase in the volume fraction of nanoparticles, the flow regime will not change. The maximum velocity is at the center of the channel, and its lowest value is near the walls; also, due to forced convection of the flow and the absence of secondary flows, the dimensionless axial velocity is symmetrical to the horizontal and vertical center lines. By increasing the volume fraction of nanoparticles from 0 to 5%, the value of this number increases.

As seen in Fig. 7, at the beginning of the channel, due to the low difference in the temperature of the nanofluid and the wall temperature, the Nusselt number is high, but

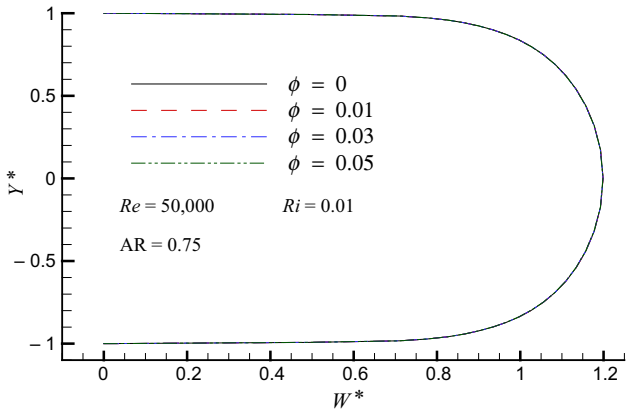

Fig. 6 Dimensionless axial velocity on a line perpendicular to the channel axis for $L/D_h = 100$

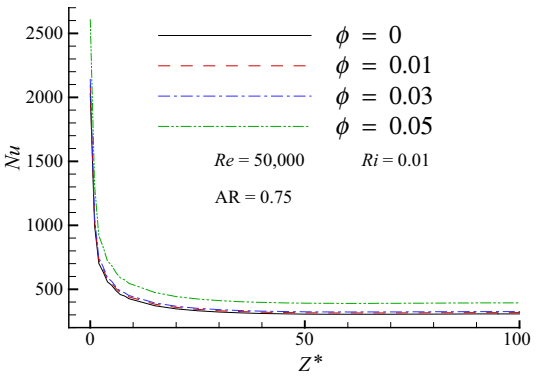

Fig. 7 Nusselt number along the channel in $L/D_h = 100$

gradually and over the channel, the temperature difference increases, and as a result, the Nusselt number decreases to reach a constant value in the developed region. The Nusselt number is the ratio of the convection to the conduction heat transfer, by increasing the volume fraction of nanoparticles, the transfer of heat convection and conduction of nanofluid increases, but the amount of increase in convection is higher than conduction.

With increasing volume fraction of nanoparticles in constant Reynolds number, the values of the physical properties of nanofluids and therefore the inlet velocity change.

Figure 8 shows variations in the mean skin friction coefficient along the channel. At the beginning of the channel, due to the high gradient velocity and therefore high shear stress, this coefficient is high but gradually decreases along the channel due to the reduction in the velocity gradient, which amounts to a constant amount during developed region. As shown in Fig. 7, with increasing volume fraction of nanoparticles, the skin friction coefficient is constant and does not change. The flow regime depends on the Reynolds number. Therefore, in the fixed Reynolds number with the change in the nanoparticle

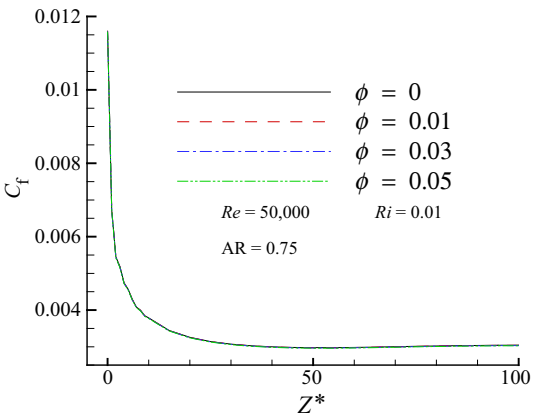

Fig. 8 Skin friction coefficient along the channel in $L/D_h = 100$

volume fraction, the mean frictional coefficient of the channel wall is constant. The coefficient of skin friction of the channel is defined as:

Aspect ratio effect on the thermal and hydrodynamic parameters

In this section, the effect of changing the aspect ratio of the channel on the thermal and hydrodynamic parameters of the nanofluid in the turbulent forced convection heat transfer is considered. In all this section, Reynolds number is 30,000 and Richardson number is 0.01. The channel is considered to have a hydraulic diameter of 0.01 m and a channel length of 100. The aspect ratio (height-to-width) of the channel has been considered in four aspect ratios of 0.25, 0.5, 0.75 and 1. Considering that in each aspect ratio the hydraulic diameter of the channel is constant, and given that the geometric characteristics of the cross section of the channels are different, the total amount of heat input is different to the channel.

In Fig. 9, the amount of dimensionless temperature increases with increasing aspect ratio. By increasing the aspect ratio for constant Reynolds and Richardson numbers, the dimesnionless temperature profiles decrease. Interaction of nanofluids dimensionless temperature and reduction in heat loss against the walls of the channel lead to an increase in the dimensionless temperature of nanofluids, by increasing the aspect ratio (Fig. 10).

In Fig. 11, due to the decrease in temperature difference with increasing aspect ratio, the amount of forced convection coefficient increases with increasing aspect ratio. In all aspect ratios, the amount of heat transfer coefficient at the beginning of the channel is high due to the low variation in wall temperature and the nanofluid temperature, but gradually decreases the value of this coefficient by moving the length of the channel due to the increase in the temperature difference until to having a constant value in the developed region. In Fig. 12, the coefficient of skin friction at the beginning of the channel is due to the high gradient velocity, which is large and reduces in the direction of the channel's axis to a constant value in the developed hydrodynamic region. As can be seen in the figure, with increasing aspect ratio, the skin friction coefficient of the channel increases. The effects of the geometry of the cross section of flow can increase the coefficient of skin friction of the channel by increasing the aspect ratio.

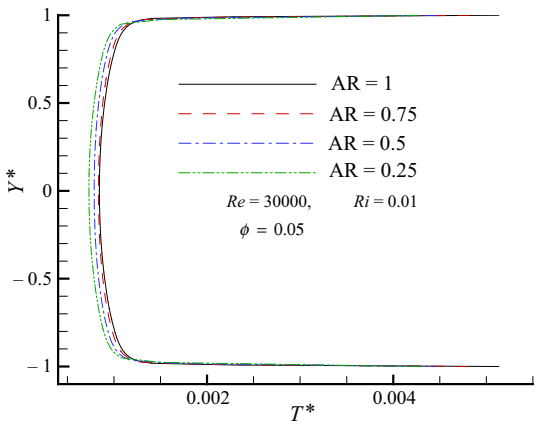

Fig. 9 Dimensionless temperature on the perpendicular line for $L/D_h = 100$

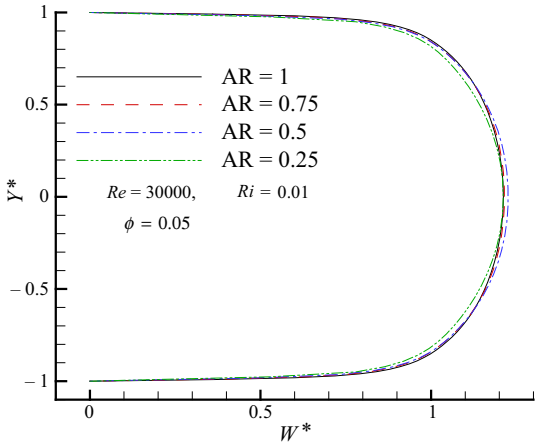

Fig. 10 Dimensionless transversal velocity for $L/D_h = 100$

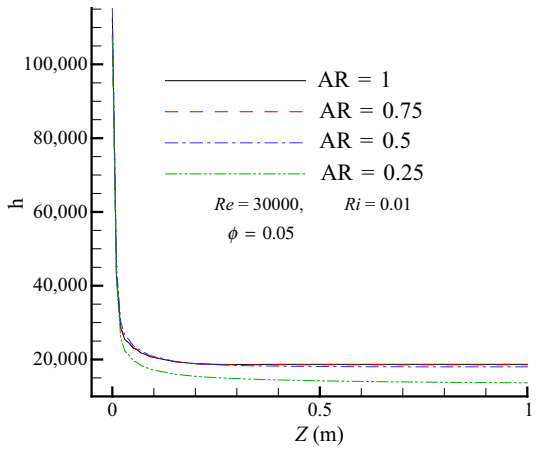

Fig. 11 Heat transfer coefficient in $L/D_h = 100$

Effect of the nanoparticles diameter on thermal and hydrodynamic parameters

In this section, the effect of changing the diameter of the nanoparticles on thermal and hydrodynamic parameters in mixed and forced convection is investigated. This study has been done in a 3% volume fraction and a diameter of nanoparticles of 20, 30 and 90 nm. The inlet temperature is

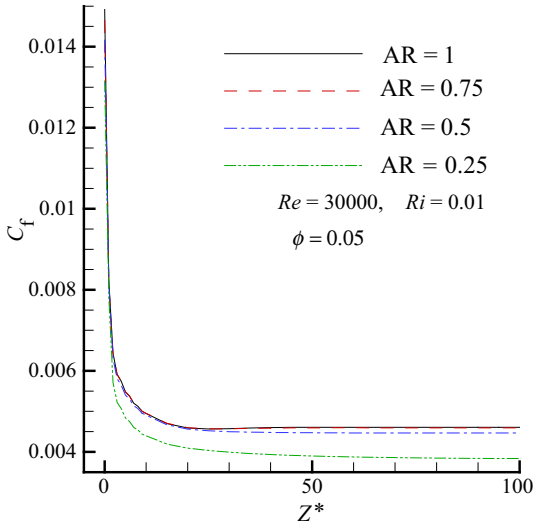

Fig. 12 Friction coefficient along the channel for L/D_h = 100

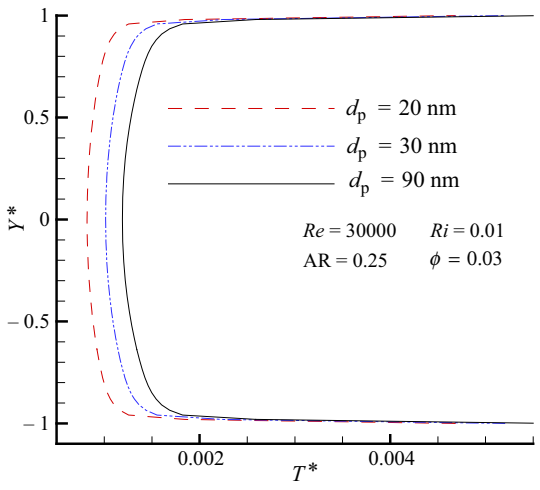

Fig. 14 Dimensional temperature variations on the perpendicular line for L/D_h = 100

assumed to be 20 °C, and the input properties are considered in this temperature. To investigate the effect of nanoparticle diameter on forced convection transfer heat, the Reynolds number is 30,000 and the Richardson number is 0.01. The channel has a hydraulic diameter of 0.01 m, a 0.75 aspect ratio and a channel length of 100.

In Fig. 13, it can be seen that increasing the average diameter of nanoparticles in a constant Reynolds number, the dimensionless axial velocity does not change significantly. According to Fig. 14, with the increasing mean diameter of the nanoparticles, the thermal conductivity coefficient, the thermal constant heat flux on the walls and the nanofluid temperature are reduced, which results in an increase in the nanofluid dimensionless temperature. With the increase in the average diameter of the nanoparticles for the constant Reynolds and Richardson numbers, the Prandtl number decreases, and this leads to the thermal development that occured earlier.

It is seen in Fig. 15 that the heat convection coefficient at the beginning of the channel is high due to the gradient of its extreme temperature, and when moving in the direction of flow, the amount of heat convection coefficient decreases to reach a constant value in the developed region. It is also seen in this figure that the increase in the diameter of the nanoparticles decreases the heat convection coefficient, because with the increase in the diameter of the nanoparticles, the thermal heat flux changes on the channel walls and, consequently, the nanofluid temperature, which due to the relationship of the forced heat convection coefficient, reduces the heat convection coefficient by increasing the diameter of the nanoparticles.

In Fig. 16, variation in the coefficient of skin friction along the channel for the forced turbulent flow of nanofluid in the constant Reynolds and Richardson is shown by increasing the diameter of the nanoparticles. As shown in this figure, the skin friction coefficient in the aspect ratio of

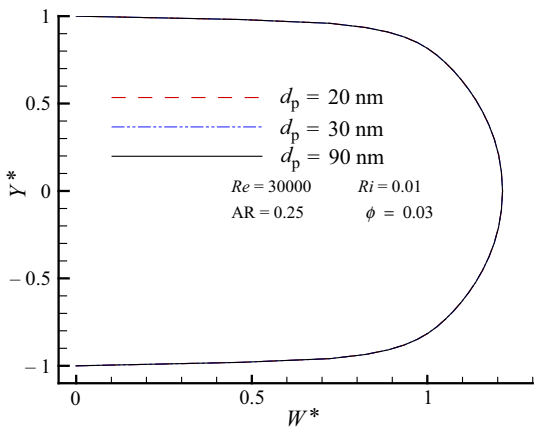

Fig. 13 Axial velocity perpendicular to axis for L/D_h = 100

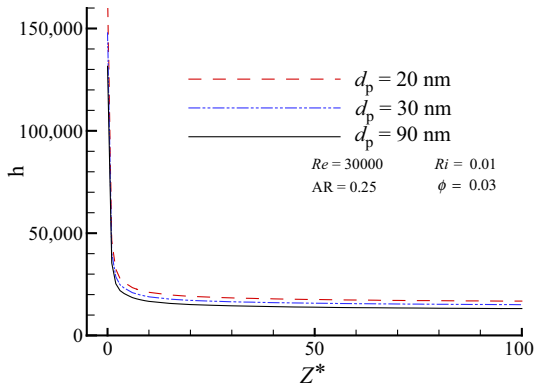

Fig. 15 Heat convection coefficient over channel length for L/D_h = 100

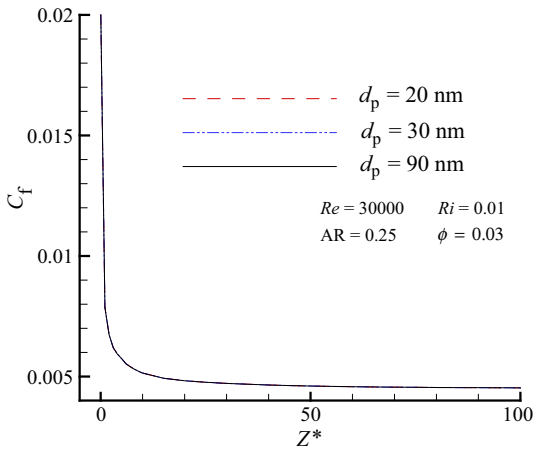

Fig. 16 Skin friction coefficient along the channel for $L/D_h = 100$

0.75 with increasing diameter of the nanoparticles has no significant changes.

Conclusions

In this study, nanofluid turbulent mixed convection of water and aluminum oxide in a three-dimensional channel with a rectangular cross section by using a two-phase mixture was analyzed. The effect of nanoparticle volume fraction on thermal and hydrodynamic parameters was studied. The results show that with increasing volume fraction of nanoparticles in constant Reynolds and Richardson number, dimensionless temperature reduces and Nusselt number increases, but dimensionless axial velocity and skin friction coefficient changes are not significant. It should be noted that in mixed convection heat transfer, the velocity and temperature profiles are not symmetrical due to the presence of secondary flow due to buoyancy force, and the minimum temperature and maximum velocity toward the wall of the bottom of the channel tend to be. About the aspect ratio, the results of this survey show that increasing the aspect ratio, the dimensionless temperature, the heat convection coefficient, Nusselt number and the skin friction coefficient of the channel increase. Also, by increasing the aspect ratio, the maximum axial velocity was not changed. In the nanoparticle diameter section, the results of this study show that in the constant volume fraction, Reynolds and Richardson number, with an increase in the mean diameter of the nanoparticles, dimensionless temperature increases and forced heat convection coefficient and the Nusselt number decrease. Also, the increase in mean diameter of nanoparticles has no significant effect on the dimensionless axial velocity and the mean skin friction coefficient of the channel.

Acknowledgements Ioan Pop would like to acknowledge the financial support received from the Grant PN-III-P4-ID-PCE-2016-0036, UEFISCDI of Romanian Ministry of Sciences. The authors wish to express their thanks to the very competent Reviewers for the very good comments and suggestions.

References

1. Maxwell JC. Treatise on electricity and magnetism. 2nd ed. Cambridge: Oxford University Press; 1904.
2. Choi SUS, Eastman JA. Enhancing thermal conductivity of fluids with Nanoparticles. In: International mechanical engineering congress and exhibition, San Francisco, CA (United States), 12–17 Nov 1995, pp 99–105.
3. Xuan Y, Li Q. Investigation on convective heat transfer and flow features of nanofluids. J Heat Transf. 2003;125:151–5.
4. Wang BX, Zhou LP, Peng XF. A fractal model for predicting the effective thermal conductivity of liquid with suspension of nanoparticles. Int J Heat Mass Transf. 2003;46:2665–72.
5. Hwang YJ, Ahn YC, Shin HS, Lee CG, Kim GT, Park HS, Lee JK. Investigation on characteristics of thermal conductivity enhancement of nanofluids. Curr Appl Phys. 2006;6:1068–71.
6. Nie C, Marlow WH, Hassan YA. Discussion of proposed mechanisms of thermal conductivity enhancement in nanofluids. Int J Heat Mass Transf. 2008;51:1342–8.
7. Sankar N, Mathew N, Sobhan CB. Molecular dynamic modeling of thermal conductivity enhancement in metal nanoparticle suspensions. Int Commun Heat Mass Transf. 2008;35:867–72.
8. Wang XQ, Mujumdar AS. Heat transfer characteristic of nanofluid: a review. Int J Therm Sci. 2007;46:1–19.
9. Ghaffari O, Behzadmehr A, Ajam H. Turbulent mixed convection of a nanofluid in a horizontal curved tube using a two-phase approach. Int Commun Heat Mass Transf. 2010;37:1551–8.
10. Rostamani M, Hosseinizadeh SF, Gorji M, Khodadadi JM. Numerical study of turbulent forced convection flow of nanofluids in a long horizontal duct considering variable properties. Int Commun Heat Mass Transf. 2010;37:1426–31.
11. Mirmasoumi S, Behzadmehr A. Effect of nanoparticles mean diameter on mixed convection heat transfer of a nanofluid in a horizontal tube. Int J Heat Fluid Flow. 2008;29:557–66.
12. Goodarzi M, Safaei MR, Vafai K, Ahmadi G, Dahari M, Kazi SN, Jomhari N. Investigation of nanofluid mixed convection in a shallow cavity using a two-phase mixture model. Int J Therm Sci. 2014;75:204–20.
13. Garoosi F, Rohani B, Rashidi MM. Two-phase mixture modeling of mixed convection of nanofluids in a square cavity with internal and external heating. Powder Technol. 2015;275:304–21.
14. Armaghani T, Chamkha AJ, Maghrebi MJ, Nazari M. Numerical analysis of a nanofluid forced convection in a porous channel: a new heat flux model in L.T.N.E. condition. J Porous Media. 2014;17:637–46.
15. Maghrebi MJ, Nazari M, Armaghani T. Forced convection heat transfer of nanofluids in a porous channel. Transp Porous Media. 2012;93:401–4013.
16. Baqaie AS, Talebi F, Armaghani T, Pop I. Numerical study of forced convection flow and heat transfer of a nanofluid flowing inside a straight circular pipe filled with a saturated porous medium. Eur Phys J Plus. 2016;131:78–88.
17. Armaghani T, Maghrebi MJ, Chamkha AJ, Al-Mudhaf AF. Forced convection heat transfer of nanofluids in a channel filled with porous media under local thermal non-equilibrium condition with three new models for absorbed heat flux. J Nanofluids. 2017;6:362–7.

18. Armaghani T, Maghrebi MJ, Chamkha AJ, Nazari M. Effects of particle migration on nanofluid forced convection heat transfer in a local thermal non-equilibrium porous channel. J Nanofluids. 2014;3:51–9.
19. Nazari M, Maghrebi MJ, Armaghani T, Chamkha Ali J. New models for heat flux splitting at the boundary of a porous medium: three energy equations for nanofluid flow under local thermal nonequilibrium conditions. Can J Phys. 2014;92:1312–9.
20. Rashidi MM, Vishnu Ganesh N, Abdul Hakeem AK, Gang B. Buoyancy effect on MHD flow of nanofluid over a stretching sheet in the presence of thermal radiation. J Mol Liq. 2014;198:234–8.
21. Rashidi MM, Abelman S, Freidooni Mehr N. Entropy generation in steady MHD flow due to a rotating porous disk in a nanofluid. Int J Heat Mass Transf. 2013;62:515–25.
22. Sheikholeslami M, Vajravelu K, Rashidi MM. Forced convection heat transfer in a semi annulus under the influence of a variable magnetic field. Int J Heat Mass Transf. 2016;92:339–48.
23. Sheikholeslami M, Rashidi MM, Hayat T, Ganji DD. Free convection of magnetic nanofluid considering MFD viscosity effect. J Mol Liq. 2016;218:393–9.
24. Hejazian M, Moraveji MK, Beheshtia AR. Comparative study of Euler and mixture models for turbulent flow of Al_2O_3 nanofluid inside a horizontal tube. Int Commun Heat Mass Transf. 2014;52:152–8.
25. Das SK, Choi SUS, Yu W, Pradeep Y. Nanofluids: science and technology. New Jersey: Wiley; 2008.
26. Nield DA, Bejan A. Convection in porous media. 4th ed. New York: Springer; 2013.
27. Shenoy A, Sheremet M, Pop I. Convective flow and heat transfer from wavy surfaces: viscous fluids, porous media and nanofluids. New York: CRC Press, Taylor & Francis Group; 2016.
28. Buongiorno J, et al. A benchmark study on the thermal conductivity of nanofluids. J Appl Phys. 2009;106:1–14.
29. Kakaç S, Pramuanjaroenkij A. Review of convective heat transfer enhancement with nanofluids. Int J Heat Mass Transf. 2009;52:3187–96.
30. Wong KFV, Leon OD. Applications of nanofluids: current and future. Adv Mech Eng. 2010;2010:1–11.
31. Manca O, Jaluria Y, Poulikakos D. Heat transfer in nanofluids. Adv Mech. Eng. 2010. Article ID 380826.
32. Mahian O, Kianifar A, Kalogirou SA, Pop I, Wongwises S. A review of the applications of nanofluids in solar energy. Int J Heat Mass Transf. 2013;57:582–94.
33. Sheikholeslami M, Ganji DD. Nanofluid convective heat transfer using semi analytical and numerical approaches: a review. J Taiwan Inst Chem Eng. 2016;65:43–77.
34. Myers TG, Ribera H, Cregan V. Does mathematics contribute to the nanofluid debate? Int J Heat Mass Transf. 2017;111:279–88.
35. Schiller L, Neumann A. A drag coefficient correlation. Z Ver Deutsch Ing. 1935;77:318–20.
36. Shah RK, London AL. Laminar flow forced convection in ducts, a source book for compact heat exchanger analytical data. New York: Academic Press; 1978.
37. Dittus FW, Boelter LMK. Heat transfer in automobile radiator of the tubular type. University of California at Berkley Publications in Engineering, vol 2. 1930. P. 443–61.
38. Cebeci T, Cousteix J. Modeling and computation of boundary-layer flows. Berlin: Springer; 2005.